Original scientific paper
Received:10.09.2025
Accepted:10.11.2025
UDC: 676.278.03-037.86:620.193.19

NUMERICAL ANALYSIS OF MOISTURE TRANSPORT IN CLT

Jan Tippner[1], Barbora Vojáčková[1], Richard Slávik[1], Pavlína Suchomelová[1]

Mendel University in Brno, Czech Republic,
Faculty of Forestry and Wood Technology,
e-mail: jan.tippner@mendelu.cz; barbora.vojackova@mendelu.cz;
richard.slavik@mendelu.cz; pavlina.suchomelova@mendelu.cz

ABSTRACT

Structural components made from wood and natural fibres are popular due to their favourable mechanical and physical properties, as well as their environmental benefits across the life cycle. However, the use of wood-based structural elements introduces risks, particularly related to increased moisture content and coupled mechanical loading.

The COMET Module project i3Sense aims to develop integrated sensing systems for monitoring key parameters such as moisture content, mechanical strain, and temperature within wood-based composites and structures. One of the project's tasks is the optimisation of the sensor placement in relation to the distribution of physical fields.

To support optimisation, a physical analysis based on numerical simulation of moisture transport is being conducted. The modelling approach differentiates moisture behaviour beneath and above the fibre saturation point by utilising diffusion and permeability coefficients. Finite element models are implemented in the COMSOL Multiphysics software.

Keywords: finite element method, moisture diffusion, free water movement, CLT panels.

1. INTRODUCTION

Wood and wood-based composites, particularly cross-laminated timber (CLT), are increasingly used in structural engineering due to their favourable mechanical performance and environmental benefits across the life cycle (Ramage et al., 2017). However, wood's variable, hygroscopic, anisotropic, and heterogeneous nature poses challenges in predicting its long-term structural behaviour under varying environmental conditions. Changes in moisture content (MC) strongly influence wood's durability, mechanical properties, dimensional stability, and susceptibility to cracking, particularly when combined with thermal and mechanical loads (Siau, 1995; Hameury, 2005).

Moisture transport in wood involves complex multi-phase interactions between free water, bound water in the cell wall, and water vapour. Bound water diffusion predominates below the fibre saturation point (FSP), while capillary-driven transport and free water movement become crucial above the FSP (Autengruber et al., 2020). This transition introduces nonlinearity and coupling effects that significantly affect the accuracy of predictive models (Trcala, 2012).

Numerical modelling has been employed to describe such transport phenomena. Early approaches were rooted in macroscopic laws, applying Fick's law for mass diffusion and Fourier's law for heat transfer (Babiak, 1995; Sherwood, 1929). Later developments introduced multiphysical frameworks based on irreversible thermodynamics (Luikov, 1966; Whitaker, 1977), enabling the inclusion of coupled hygrothermal effects such as thermo-diffusion (Soret effect) and heat flux induced by water migration (Dufour effect) (Avramidis et al., 1992; Lewis and Ferguson, 1993). While these approaches

advanced a modelling approach, they often relied on back-calculated material parameters that lacked clear physical meaning, thereby limiting generalisation (Eitelberger and Hofstetter, 2011).

Recent research has introduced significant refinements and applications to wood-based composites. Brandstätter et al. (2024) demonstrated, via two-dimensional simulations, how geographic factors and altitude influence MC distributions in CLT, directly linking moisture gradients to cracking risk and highlighting shortcomings of current standards. Anisotropic hygrothermal modelling by Kalbe et al. (2024) introduced a performance criterion for end-grain moisture safety in CLT, addressing challenges during construction and exposure. Wang et al. (2023) validated hygrothermal models with field data on CLT end-grain exposure, underscoring the need for precise calibration of moisture storage functions and water absorption coefficients. Beyond pure hygrothermal modelling, a coupled moisture–mechanical study (Sun et al., 2025) integrates mechano-sorptive creep and examines long-term deformation of CLT under humidity variations.

The FFG COMET Module project *i3Sense* (I*ntelligent, integrated, and impregnated cellulose-based sensors for reliable bio-based structures*) aimed to develop integrated sensing systems for monitoring key parameters such as moisture content, mechanical strain, and temperature in wood-based composites. One of the tasks is the optimisation of sensor placement in relation to evolving physical fields. We perform numerical simulations of moisture transport in CLT utilising a split technique to facilitate this, differentiating between bound-water diffusion below FSP and permeability-driven flow above FSP. Numerical models of moisture transport are implemented using finite-element frameworks in COMSOL Multiphysics.

2. MATERIAL AND METHODS

2.1. Experiment

To investigate moisture transport mechanisms and validate numerical models at the material level, an experiment was conducted using two sets of small spruce (*Picea abies* (L.) H. Karst) and beech (*Fagus silvatica* L.) samples. Each set consisted of four specimens with dimensions of 0.02 × 0.02 × 0.3 m (Fig. 1).

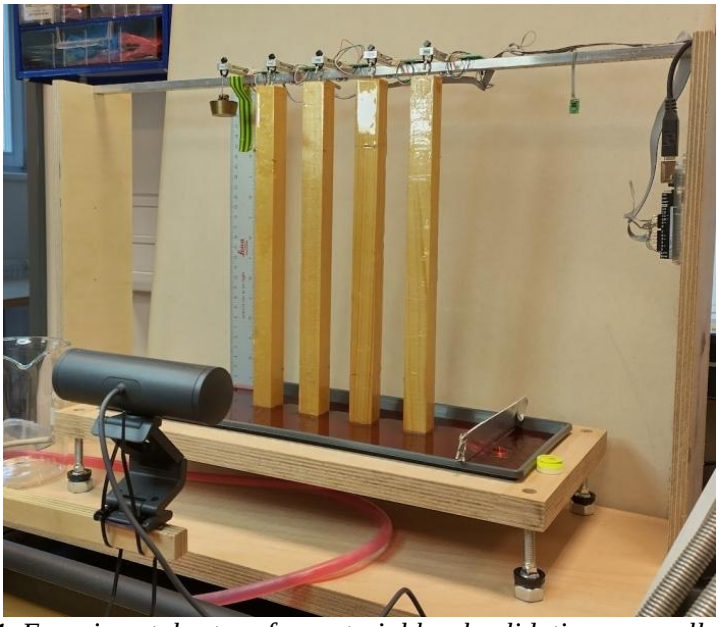

Figure 1. *Experimental set-up for material level validation on small samples.*

The samples were suspended vertically with their lower ends submerged in water. Mass gain of samples and their environmental conditions (temperature and relative humidity) were monitored by a multi-channel board (Atmel328 microcontroller, Microchip Technology Inc., USA) and sensors (SENSIRION SHT21, Mouser Electronics Inc., USA).

The first set of samples had their side walls coated with epoxy resin, restricting the exchange of moisture with the environment. This setup was designed to simulate one-dimensional moisture flow along the longitudinal axis of the wood. The second set remained untreated, with open side walls, allowing for multidirectional moisture exchange. The water level in the soaking container was maintained at a constant height throughout the experiment. The samples were monitored over a period of 27 days.

In light of the orthotropic nature of wood and the combined effects of moisture diffusion below the FSP, free water movement (above FSP), and moisture exchange with the environment through the surfaces, the experiment yielded data for calibration and validation of numerical models intended to simulate moisture transport in wood.

To gain an understanding of moisture transport in cross-laminated timber (CLT) panels, two samples (dimensions: 0.9 × 0.2 × 0.1 m) were subjected to a water soaking experiment. Each sample was suspended vertically with its bottom edge submerged in water for a period of 11 days. During this time, ambient air humidity and temperature and the mass of samples were continuously monitored.

Eight sensors (SENSIRION SHT21, Mouser Electronics Inc., USA) were installed on each sample at three positions (two on the sides and one in the centre) along the panel length (Fig. 2). Two additional sensors were placed in the surrounding environment to monitor ambient conditions. Data acquisition was performed using a multi-channel board (Atmel328 microcontroller, Microchip Technology Inc., USA).

Sample A had open side walls, allowing moisture transfer in all directions and exchange between the air environment and the sample. Sample B had its side walls sealed with aluminium foil, restricting transport to the front and back surfaces only. The water level in the soaking container was maintained at a constant height throughout the experiment.

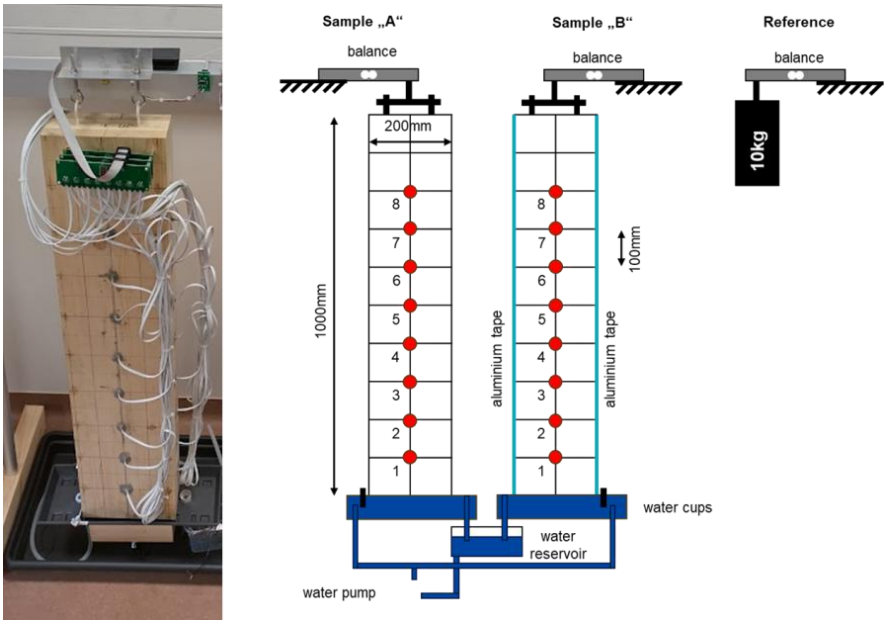

Figure 2. *Set-up for water uptake monitoring of CLT samples.*

2.2. Numerical modelling

A numerical model of coupled moisture transport below and above FSP, using separate diffusion and permeability coefficients for each regime, was developed using COMSOL Multiphysics version 6.2 (COMSOL AB, Sweden), a simulation platform based on the finite element (FE) method.

Using a method similar to that outlined by Suchomelová et al. (2019), a three-dimensional (3D) model was constructed with governing equations implemented via the Partial Differential Equation (PDE) interface. Moisture transport was modelled as a combined process, integrating both moisture diffusion and free-water movement. Moisture diffusion (M_d), driven by concentration gradient and described by Fick's law, uses diffusion coefficients (D, eq. 1). For the movement of free water (M_f),

driven by pressure gradients, the equation based on Darcy's law uses the permeability coefficients (*P*, eq. 2).

$$\frac{\partial M_d}{\partial t} - \nabla(D\nabla M_d) = 0 \qquad (1),$$

$$\frac{\partial M_f}{\partial t} - \nabla\left(P\nabla M_f\right) = 0 \qquad (2),$$

The diffusion coefficients were defined as a function of MC and calculated to the FSP (set at 28% MC), following Suchomelová et al. (2019). The permeability coefficients are also moisture-dependent up to full saturation. The mathematical derivation of permeability coefficients was based on Autengruber et al. (2020); the permeability coefficients for longitudinal, radial, and tangential (L, R, T) directions were determined using the following equation:

$$P = K\left(-0.61\left(12400\left(\frac{M_d}{f_{lum}\rho_{H2O}}\right)^{-0.61}\right)\right)\frac{1}{M_d} \qquad (3),$$

where *K* is the absolute permeability defined by Autengruber et al. (2020); f_{lum} volume proportion of the cell lumen depending on the bound water concentration.

The geometry of the model was represented by a solid block with dimensions corresponding to the experiment (0.02 × 0.02 × 0.3 m), Fig. 3. The geometrical axes corresponded to anatomical directions (L = Z, R = Y, T = X). The maximum element size was set to 0.005 m, and the overall number of domain, boundary, and edge elements was 1180.

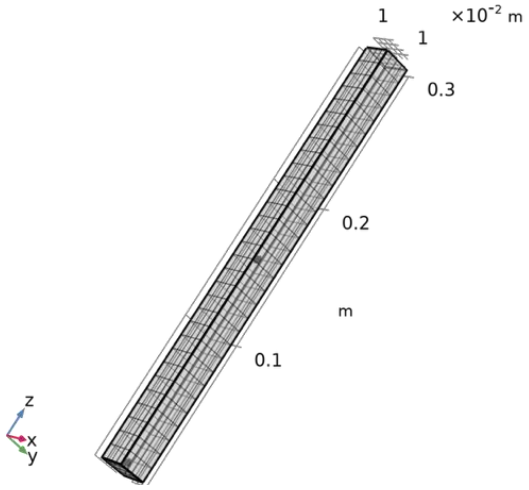

Figure 3. *FE model of solid wood sample.*

The initial conditions (MC = 1%) were assumed to be uniform throughout the entire volume. The MC value for the diffusion component of moisture transfer was set below the FSP, in accordance with experimental observations, while the free-water component was initialized at the FSP.

Boundary conditions, applied on all open walls except the bottom one (intake), were implemented using the predefined flux/source equations in COMSOL Multiphysics. Based on Suchomelová et al. (2019), the adsorption/impedance term was defined by the moisture transfer coefficient (α_M), and the flux/source term was defined as α_M multiplied by potential equilibrium moisture content (EMC) corresponding to the ambient environment conditions (temperature, humidity) during the experiment. The Dirichlet boundary conditions were applied on the bottom wall (intake). The solution was a time-dependent nonlinear one, with a time step of 600 s, and the integrated solver MUMPS was used.

The default range of selected basic physical parameters for the testing of material models of spruce and beech were oven-dry density: 516 / 705 kg.m^{-3}; moisture transfer coefficient (α_M): 5.10^{-6} - 5.10^{-9} m^{-1}; longitudinal diffusion coefficient (D_L): 2.10^{-8} - 2.10^{-9} (-); transversal diffusion coefficient (D_T): 1.10^{-9} - 1.10^{-11} (-); longitudinal permeability coefficient (P_L): 2.10^{-2} - 2.10^{-6} g.m^{-9}; and transversal permeability coefficients (P_T): 2.10^{-2} - 2.10^{-6} g.m^{-9}. However, full orthotropy with MC dependency was defined.

The equation-based prescription of MC dependencies for all material and boundary conditions parameters was used in the COMSOL Multiphysics environment. The calibrated and validated physical model of solid wood response was adopted for a 3D model of a CLT panel sample with the dimensions, boundary conditions, and initial conditions corresponding to the experiment. The geometry of the model was represented by three interacting solid-block layers with overall dimensions corresponding to the experimental CLT sample (0.9 × 0.2 × 0.1 m), Fig. 4. The geometrical axes corresponded to anatomical directions of layers (L = Z, R = Y, T = X for two outer surface layers; L = X, R = Z, T = Y for the inner layer). The interaction between layers (bond line) was simplified to fully coupled regions (shared FE nodes), and the complex influence of the bond line was simplified and represented by calibrated material parameters of wood. The maximum element size was set to 0.01 m, and the overall number of domain, boundary, and edge elements was 7992. The solution was realized as a time-dependent nonlinear (12 days in total), with a time step of 20 minutes, and the integrated solver MUMPS was used.

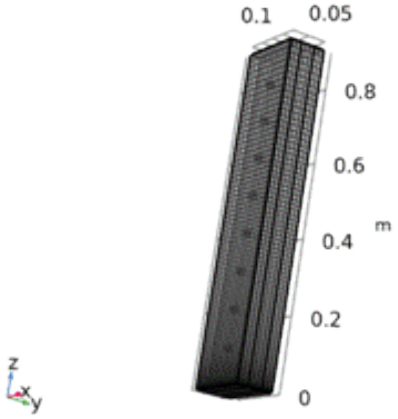

Figure 4. *FE model of CLT sample.*

3. RESULTS AND DISCUSSION

The experimental evaluation was based on mass recording. The change of MC was calculated in principle of the gravimetric method and represented by time-history plots. Typical postprocessing outputs from FE simulation consist of a) nodal contour plots of MC distribution and b) time-history listing of MC values-local (nodal) values and average values calculated for selected regions. These outputs were used for experimental validation.

3.1. Small sample model validation

Fig. 5 illustrates the development of MC distribution in three time steps, where the region with higher values of MC, even in later periods, shows evident distribution restrictions to the area close to the intake of water.

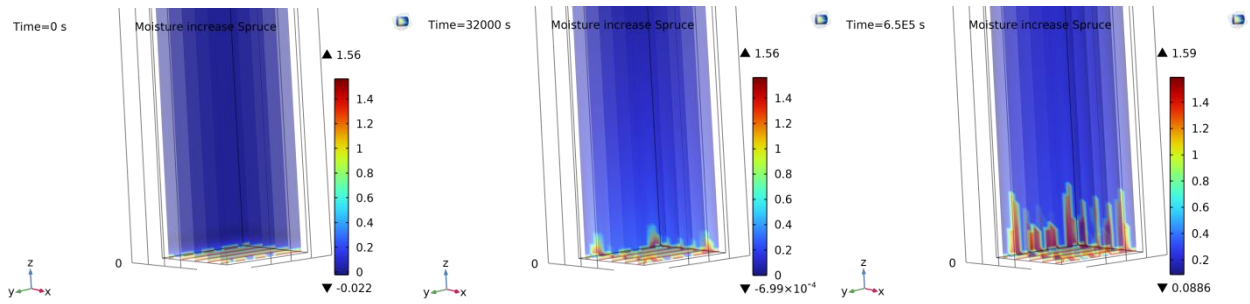

Figure 5. *Nodal solution of MC in 0 seconds, 9 hours, and 7.5 days.*

Fig. 6 shows the behaviour of small-sample models for beech and spruce under different initial conditions and boundary conditions. The time history of a) bound water – increasing MC from 5% to 15%, b) bound water – decreasing MC from 15% to 5%, and c) mixed free and bound water – increasing MC from 5% to 18% shows a physically consistent response in drying, wetting, and soaking water. The consistent transversal distribution of MC in transient tasks is then confirmed by comparing MC development on the surface and within the sample (d).

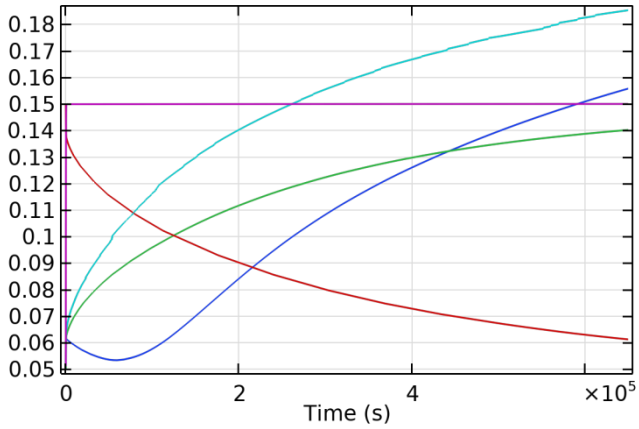

Figure 6. *Verification of small-sample model with different initial and boundary conditions. Average MC (-) for spruce: red curve - drying, green - wetting, cyan - wetting + soaking (for which the violet is from the surface and the blue from the middle of the sample).*

The influence of moisture exchange with the environment, represented by αM, was tested on the responses of FE models by closing lateral walls. The insulation also has an impact on the anisotropy of water transport in solid (3D to one-directional). For the insulated case, an increase of moisture uptake, at 7.5 days, is about 31% higher for beech and 48% for spruce (Fig. 7).

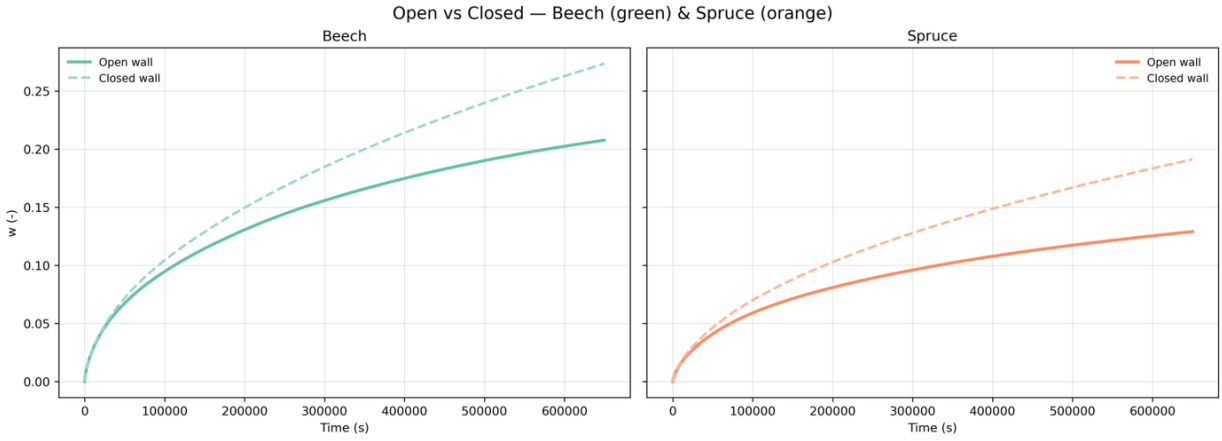

Figure 7. *Verification of the influence of boundary conditions for beech (green) and spruce (orange). Solid lines – open wall with transfer to air environment; dashed line – closed wall (insulated by resin).*

The experimentally observed MC increase for spruce with open walls (not treated with resin) over 7.5 days was 13%, with very low variability. For beech, there was a 20% MC increase, but with higher variability among the samples (Fig. 8). Two samples showed an increase in MC similar to spruce (11% and 13% MC change), while two others exhibited much higher values (27% and 43%). This variability in moisture uptake is particularly interesting because the variability in density of the small samples was low (coefficient of variation: 5% for spruce and only 2% for beech). Additionally, the

samples were visually identical (fibre orientation, annual ring thicknesses) and of excellent quality (defect-free, regular structure), indicating that chemical or microscopic elements might be important.

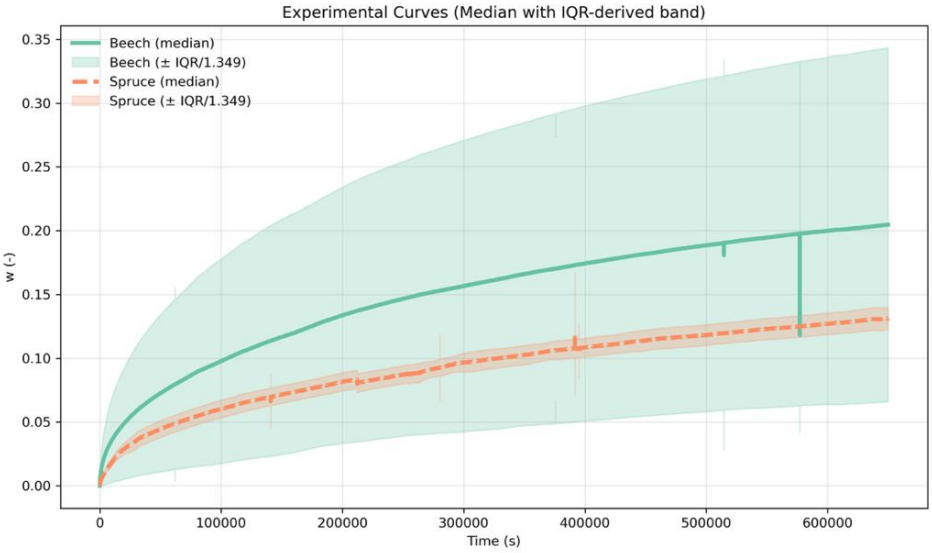

Figure 8. *Experimental validation – time history of MC for spruce (orange) and beech (green) with corresponding intervals of variability.*

The FE model of the MC increase in spruce required calibration. This was achieved through a sensitivity analysis (500 loop computations for testing of input parameters, Fig. 8), in which the optimised values of parameters included the moisture transfer coefficient (α_M), permeability coefficients (P_L, P_R, P_T), and diffusion coefficients (D_L, D_R, D_T), all in the longitudinal, radial, and tangential directions. The parameters with significant influence were α_M, P_L, and D_L. The best-fit model yielded an α_M of 5×10^{-9} m^{-1}, a P_L ranging from 0.0014×10^5 and exponentially decreasing to 0.0001×10^5, and a D_L exponentially increasing from 2.06×10^{-9} to 2.18×10^{-9}.

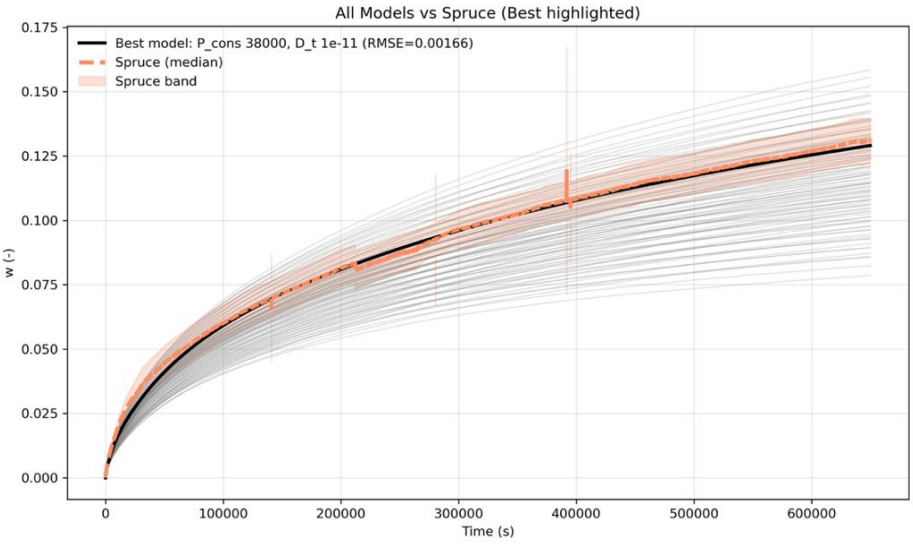

Figure 9. *Sensitivity analysis for spruce small samples – the range of FE models' responses compared to experimental records of MC.*

For beech (Fig. 9), the calibration was mainly concentrated on the properties which differ from spruce, and the sensitivity analysis contains only 20 computations. DT was used to calibrate PL, DL,

and DR. P_L ranging from 0.0055 and exponentially decreasing to 0.0004, and a D_L exponentially increasing from 2.06×10^{-8} to 2.18×10^{-8}, and D_R 4.2×10^{-10} to 5.8×10^{-10}.

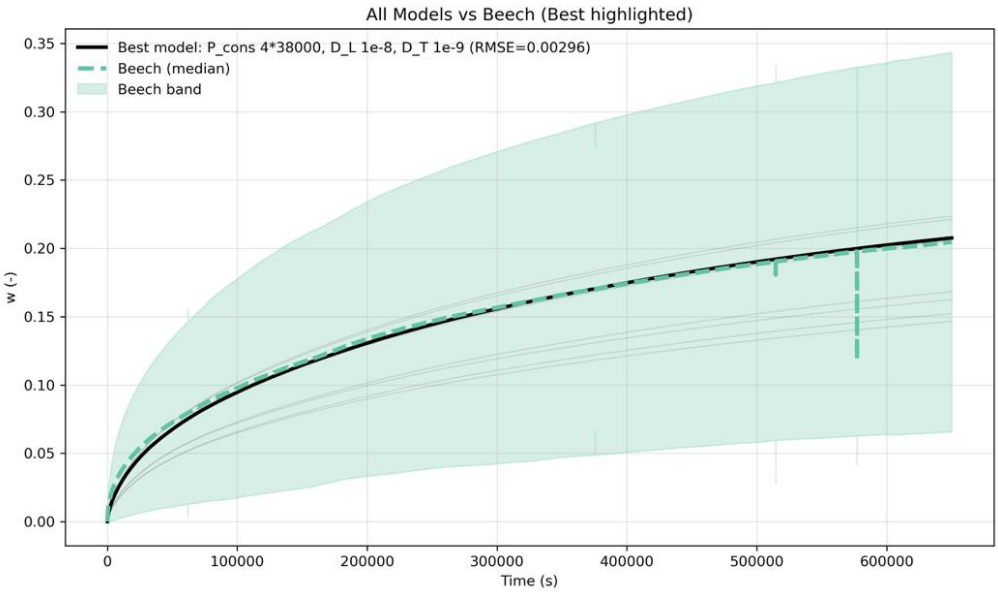

Figure 10. *Sensitivity analysis for beech small samples – the range of FE models' responses compared to experimental records of MC.*

3.2. CLT-sample model validation

Fig. 11 illustrates experimentally evaluated distributions of MC in CLT samples for case studies with different boundary conditions (open or closed by non-permeable insulation on lateral sides). The highly variable original data were filtered; the smooth MC distributions show 1) comparable MC values between lateral sensors, 2) differences between centre and lateral sensors, and 3) a consistent increase of MC of all sensors in time. The closed samples show 1) higher values of MC in central sensors in comparison to the closed sample, 2) higher MC values measured by central sensors in comparison to the lateral one, and 3) higher velocity of MC increase in time for the central part in comparison to less-intensive MC increase in insulated regions.

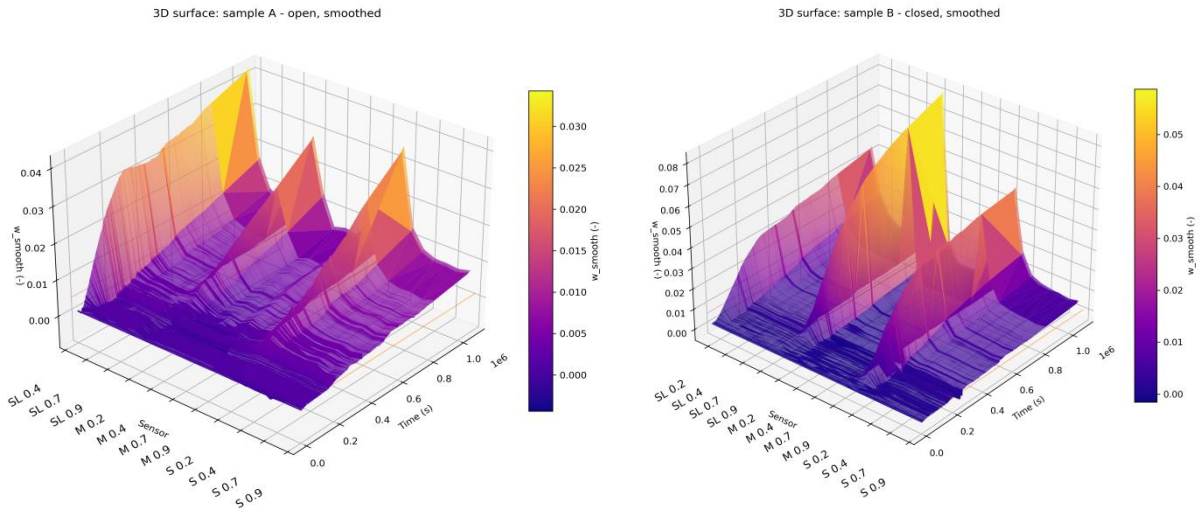

Figure 11. *Experimentally evaluated MC distribution in CLT sample – sensor values in time for open vs. closed lateral walls.*

The outputs of the numerical study of CLT samples are shown in Fig. 12 with a contour plot of the nodal solution of MC. The distribution points to a low-lying region with higher MC values, followed by a large region with MC corresponding to a common range of EMC during use of CLT construction. The sharp MC distribution with the highest gradient of MC in the region up to approx. 0.1 m is supported by a trend of experimental data (Fig. 11). A satisfactory agreement of experimental and simulation data in the time domain at the initial part of the process is illustrated in Fig. 13 too.

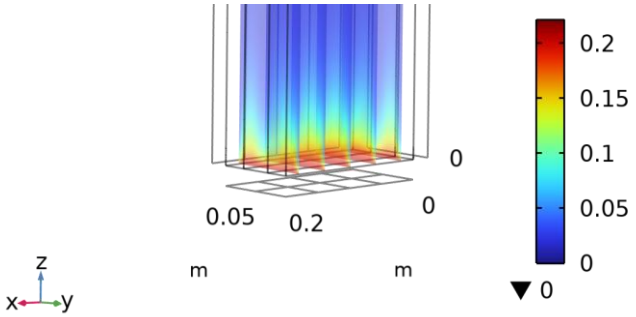

Figure 12. *Nodal solution of MC in the CLT sample, detailed distribution of the bottom of the sample in steady state (at terminating time).*

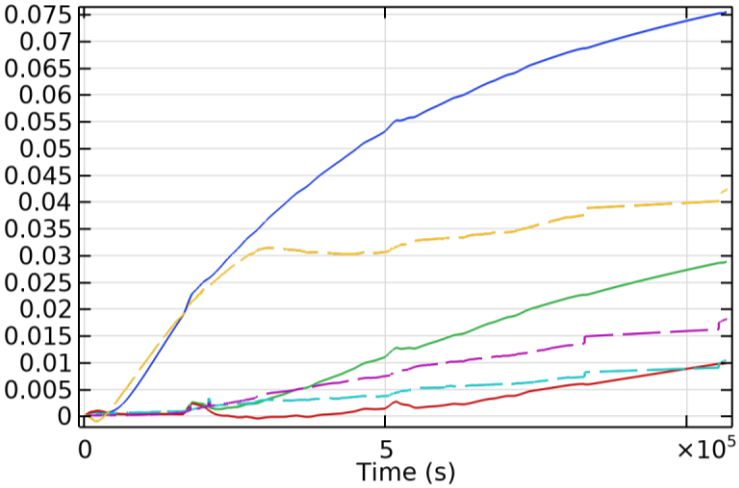

Figure 13. *Time-history plots of MC (-) in 0.1, 0.2, and 0.3 m height positions (dashed line – experimental values, solid line – FE model).*

4. CONCLUSIONS

The FE transient simulation in COMSOL Multiphysics software successfully predicted moisture transport in wood, considering its orthotropic nature, coupled effects of moisture diffusion below FSP, free-water movement above FSP, and moisture exchange between the surface and the air environment.

The process of model building based on material validation on small-scale solid wood samples and upscaling to real-scale CLT models was successfully applied.

The physical consistency of the model was verified by testing alternating scenarios 1) with/without water intake (moisture movement above/below FSP) and 2) different initial conditions (MC) and boundary conditions (air humidity and temperature), inducing an increase or decrease of EMC.

The verified model with consistent physical response under different scenarios was calibrated and experimentally validated for 2 materials (spruce and beech solid wood). The experiment of

longitudinal water soaking of small solid wood samples (0.02 × 0.02 × 0.3 m) was used for the validation.

A material model was applied to a case study of a 3-layered CLT. The numerical model of the CLT sample (0.9 × 0.2 × 0.1 m) water soaking was experimentally validated at 2 scenarios of environment boundary conditions (open or closed lateral sides). The validated model of CLT brought a time-dependent 3D description of MC distribution. Results show a high gradient of MC in the bottom region of the sample (close to contact with the water level) and a relatively homogeneous response in regions above the 0.1 m level. This behaviour should be respected in the design of sensors and their placement and data interpretations during CLT construction monitoring as well.

The FE model of CLT was used for what-if scenarios covering changes of material parameters (parameters' variability, anisotropy ratios), initial conditions (MC) and boundary conditions (air humidity). The response was highly influenced by the alteration of transfer coefficients (αM), longitudinal dinal diffusion coefficient (DL) and longitudinal permeability coefficient (P_L).

Based on MC outputs, the several types of regions relevant to sensor placement can be recognised: the bottom region (below 0.05 - 0.1 m) with MC above FSP, the region about FSP, the region with increased MC (easily detectable by sensors), and the large region (above approx. 0.3 m) with MC varying in a common range, which corresponds naturally to oscillations during the year, where the detection can be complicated.

Next research aims to 1) add geometry-defined glue-line regions, 2) add full structure composition (wall layers and connections), 3) involve in-situ environment parameters in long-term life cycle, 4) use a probabilistic approach dealing with variability of materials and conditions, and 5) apply models for in-practice monitoring during water-hazard incidents.

ACKNOWLEDGMENT

This work has been supported by the COMET module project "i3sense" (Intelligent, integrated and impregnated cellulose-based sensors for reliable biobased structures, project number: FO999888361) funded by the Austrian ministries BMK and BMAW and the federal states of Upper Austria, Lower Austria, and Carinthia, operated by the FFG.

REFERENCES

1. Autengruber, M., Lukacevic, M., Füssl, J. (2020): Finite-element-based moisture transport model for wood including free water above the fiber saturation point. International Journal of Heat and Mass Transfer, 161:120228.
2. Avramidis, S., Englezos, P., Papathanasiou, T. (1992): Dynamic Nonisothermal Transport in Hygroscopic Porous Media: Moisture Diffusion in Wood. American Institute of Chemical Engineers, 38:1279–1287.
3. Babiak, M. (1995): Is Fick's law valid for the adsorption of water by wood? Wood Science and Technology, 29:227–229.
4. Brandstätter, F., Autengruber, M., Lukacevic, M., Füssl, J. (2024): The influence of geographical location on moisture distribution in wood cross sections: a numerical simulation study using Austria as an example. Journal of Wood Science 70(1):35.
5. Kalbe, K., Kalamees, T., Kukk, V., Ruus, A., Annuk, A. (2022): Wetting circumstances, expected moisture content, and drying performance of CLT end-grain edges based on field measurements and laboratory analysis, Building and Environment, 221:109245.
6. Eitelberger, J., Hofstetter, K. (2011): A comprehensive model for transient moisture transport in wood below the fiber saturation point: Physical background, implementation and experimental validation. International Journal of Thermal Sciences, 50(10):1861–1866.
7. Hameury, S. (2005): Moisture buffering capacity of heavy timber structures directly exposed to an indoor climate: A numerical study. Building Environment 40(10):1400–1412.
8. Lewis, R.W., Ferguson, W.J. (1993): A partially nonlinear finite element analysis of heat and mass transfer in a capillary-porous body under the influence of a pressure gradient. Applied Mathematical Modelling, 17(1):15-24.

9. Luikov, A.V. (1966): HEAT AND MASS TRANSFER IN CAPILLARY-POROUS BODIES, in: Heat and Mass Transfer in Capillary-Porous Bodies. Elsevier, pp. 233–303.
10. Ramage, M.H., Burridge, H., Busse-Wicher, M., Fereday, G., Reynolds, T., Shah, D.U., Wu, G., Yu, L., Fleming, P., Densley-Tingley, D., Allwood, J., Dupree, P., Linden, P.F., Scherman, O. (2017): The wood from the trees: The use of timber in construction. Renewable and Sustainable Energy Reviews, 68(1):333-359.
11. Sherwood, T.K. (1929): The Drying of Solids-I. Industrial & Engineering Chemistry, 21(1):12–16.
12. Siau, J.F. (1995): Wood: Influence of Moisture on Physical Properties. Virginia Poly Institute and State University, Blacksburg.
13. Suchomelová, P., Trcala, M., Tippner, J. (2019): Numerical simulations of coupled moisture and heat transfer in wood during kiln drying: Influence of material nonlinearity. Bioresources, 14(4):9786–9805.
14. Sun, X., He, M., Li, Z., Ou, J., Zheng, X., Wei, M. (2025): Experimental study on the long-term creep behavior of cross-laminated timber under axial compression used for mass timber structural systems, Engineering Structures 338:120644.
15. Trcala, M. (2012): A 3D transient nonlinear modelling of coupled heat, mass and deformation fields in anisotropic material. International Journal of Heat and Mass Transfer, 55(17–18):4588-4596.
16. Wang, L, Ge, H., Wang, J. (2023): Model validation and 2-D hygrothermal simulations of wetting and drying behavior of cross-laminated timber. Journal of Building Physics. 46(6):737-761.
17. Hitaker, S. (1977): Simultaneous Heat, Mass, and Momentum Transfer in Porous Media: A Theory of Drying, 13:119–203.